Spinal Cord (2021) 59:319–327
https://doi.org/10.1038/s41393-020-00571-8

ISCoS The International Spinal Cord Society

ARTICLE

Early and sustained improvements in motor function in rats after infusion of allogeneic umbilical cord-derived mesenchymal stem cells following spinal cord injury

F. M. Moinuddin[1,2] · Yagiz U. Yolcu[1,2] · Waseem Wahood[1,2] · Ahad M. Siddiqui[3] · Bingkun K. Chen[3] · Mohammed Ali Alvi[1,2] · Anshit Goyal[1,2] · Jarred J. Nesbitt[3] · Anthony J. Windebank[3] · Jiunn-chern Yeh[4] · Kathy Petrucci[4] · Mohamad Bydon[1,2]

Received: 31 March 2020 / Revised: 14 October 2020 / Accepted: 19 October 2020 / Published online: 2 November 2020

Abstract

Study design Animal study.

Objectives Umbilical cord-derived mesenchymal stem cells (UC-MSCs) have recently been shown to hold great therapeutic potential for spinal cord injury (SCI). However, majority of the studies have been done using human cells transplanted into the rat with immunosuppression; this may not represent the outcomes that occur in humans. Herein, we present the therapeutic effect of using rat UC-MSCs (rUC-MSC) without immunosuppression in a rat model of SCI.

Setting Mayo Clinic, Rochester, MN, USA.

Methods Twelve female rats were randomly divided into two groups, control, and rUC-MSC group, and then subjected to a T9 moderate contusion SCI. Next, 2×10^6 rUC-MSCs or ringer-lactate solution were injected through the tail vein at 7 days post injury. Rats were assessed for 14 weeks by an open-field Basso, Beattie, and Bresnahan (BBB) motor score as well as postmortem quantification of axonal sparing/regeneration, cavity volume, and glial scar.

Results Animals treated with rUC-MSCs were found to have early and sustained motor improvement (BBB score of 14.6 ± 1.9 compared to 10.1 ± 1.7 in the control group) at 14 weeks post injury (mean difference: 4.55, 95% CI: 2.04 to 7.06; p value < 0.001). Total cavity volume in the injury epicenter was significantly reduced in the rUC-MSC group; control: 33.0% ± 2.1, rUC-MSC: 25.3% ± 3.8 (mean difference: −7.7% (95% CI: −12.3 to −2.98); p value < 0.05). In addition, spinal cords from rats treated with rUC-MSCs were found to have a significantly greater number of myelinated axons, decreased astrogliosis, and reduced glial scar formation compared to control rats.

Conclusions Our study indicates that intravenous injection of allogenic UC-MSCs without immunosuppression exert beneficial effects in subacute SCI and thus could be a useful therapy to improve the functional capacity among patients with SCI.

Introduction

Spinal cord injury (SCI) is a debilitating insult that results in total and partial paralysis [1]. Despite extensive research and exploratory trials, there are no proven effective treatments to recover lost neurological function. Due to its complex pathophysiology, current treatments have been limited to arresting further neurological decline rather than recovery of function. Therefore, potential therapeutic agents/modalities targeting different phases of the injury have been studied in recent years [2]. Among them, cellular therapies have attracted a considerable amount of attention in the field owing to the potential to replace lost cells, enhancing regeneration, and preventing further injury [3].

Supplementary information The online version of this article (https://doi.org/10.1038/s41393-020-00571-8) contains supplementary material, which is available to authorized users.

✉ Mohamad Bydon
bydon.mohamad@mayo.edu

[1] Mayo Clinic Neuro-Informatics Laboratory, Mayo Clinic, Rochester, MN, USA

[2] Department of Neurologic Surgery, Mayo Clinic, Rochester, MN, USA

[3] Department of Neurology, Mayo Clinic, Rochester, MN, USA

[4] Animal Cell Therapies, Inc., San Diego, CA, USA

However, it is hard to determine the optimal type, source, condition of cells, as well as optimal treatment time for different injury levels, severity and/or phases of SCI. Previously, cells derived from the central nervous system (such as neural stem cells and oligodendrocyte progenitor cells) and other tissues such as embryonic stem cells, Schwann cells, Olfactory Ensheathing Cells, induced pluripotent stem cells, and mesenchymal stem cells (MSCs) have frequently been tested for their impact on recovery [3–5]. MSCs are isolated from various tissues with bone marrow, adipose tissue, and umbilical cord being the most common. While bone marrow and adipose tissue derived MSCs can be obtained as autologous cells, they require an invasive procedure for cell preparation [6]. Currently, the role of MSCs is being investigated in clinical trials (NCT03308565). However, isolation, expansion, and characterization autologous cells may not always be feasible for every patient and there may be instances where a prepared product is needed. Umbilical cord-derived mesenchymal stem cells (UC-MSCs) are easier to isolate and expand with few ethical considerations, exhibit greater proliferative activity, and do not require an invasive procedure for the patient [7]. These properties make umbilical cord cells ideal for the current practice of stem cell banking.

In previous preclinical studies, UC-MSCs have been associated with improved local angiogenesis, reduction of glial scar formation by upregulating metalloproteinases and inhibiting inflammatory cell infiltration following SCI [8–10]. Therefore, more research on the effectiveness of intravenous delivery of UCMSC in SCI is warranted. Finally, most studies previously performed transplanted human cells in immunosuppressed rats. The outcomes of such studies may not be entirely representative of humans since it is not clear how transplanted cells may be impacted by use of immunosuppressive drugs in humans. Therefore, further optimization of cellular treatment without the need for immunosuppression is required, especially given the long-term impact on recovery and the short life span of these cells. Herein, we investigated the efficacy of intravenous UCMSC injections on histopathological and functional outcomes in a rat model of traumatic SCI with long-term (14 week) follow-up in immunocompetent rats.

Methods

Isolation and culture of rat umbilical cord-derived mesenchymal stem cells (rUC-MSCs)

Umbilical cord MSCs were isolated and cultured by Animal Cell Therapies, Inc. (San Diego, CA) and transferred to Mayo Clinic on the same day of administration. Briefly, fresh rat umbilical cords were obtained from full term pregnant Sprague-Dawley rats using sterile instruments and techniques. The umbilical cords were washed with Hank balanced salt solution containing penicillin/streptomycin/amphotericin B until mostly blood free. After washing, the cords were cut into small pieces and digested with an enzyme solution containing collagenase/hyaluronidase at 37 °C with gentle rocking. The digested mixture was then passed through a 100 µm cell strainer to obtain cell suspensions. The released cells were pelleted by centrifugation and seeded in cell culture vessels. Cells were cultured with proprietary culture medium optimized for UC-MSCs at Animal Cell Therapies that was based on a DMEM (ThermoFisher)/MCDB (Sigma)-based medium supplemented with 5% FetalClone III (HyClone) and growth factors. Nonadherent cells were removed by changing the media day after seeding. Adhered cells (passage one) were harvested when reaching 80–90% confluency. The harvested cells were seeded in 10 cm culture dish and maintained using standard cell culture techniques. Passage two cells were tested for cell viability and possible contamination (IDEXX IMACT IV panel, Columbia, MO) before using for the study.

Characterization of rUC-MSCs

To determine the purity of rUC-MSCs we analyzed the expression of cell surface markers by flow cytometry analysis. In total, 3×10^4 to 10^5 passage 2 cells were used for each antibody. Cells stained with isotypic antibody and the same fluorescence conjugate were used as the control. After washing, cells were analyzed on a FACSCalibur™ (BD Biosciences) using CellQuest Pro software. Antibodies used for staining included: mouse antirat CD44-PE (eBioscience), mouse antirat CD45-FITC (eBioscience), mouse antirat MHC II-FITC (eBioscience), and mouse antimouse/rat CD90-PE (eBioscience). Anti-isotypic control antibodies used were PE-conjugated mouse IgG2a kappa isotype control antibody (BioLegend) for anti-CD44-PE and anti-CD90-PE, and FITC-conjugated mouse IgG1 kappa isotype control antibody (eBioscience) for anti-CD45-FITC and anti-MHC II-FITC. To ensure the high purity of rUC-MSCs, we used cells which were 95% positive for CD44, 96% positive for CD90 and negative for CD45 (1% positive) and MHC II (less than 1% positive; Supplementary Fig. 1).

For differentiation potential, rUC-MSCs were seeded and induced using StemPro differentiation kits for adipogenesis and osteogenesis (Gibco, Invitrogen, USA) according to manufacture protocols with minor modifications. Cells grown in regular culture medium served as negative controls. For adipocyte differentiation, adipogenic-induced rUC-MSCs stained positive for oil red O. For osteocyte differentiation, osteogenic-induced rUC-MSCs stained positive for Alizarin red S (ARS) which binds to the

calcium deposits when differentiated osteocytes mineralize the extracellular matrix. The control cells from neither group stained positive with the respective dye (Supplementary Fig. 2).

Animal model

All animal protocols were approved by the Mayo Clinic Institutional Animal Care and Use Committee and complied with guidelines from the National Institutes of Health. Adult female Sprague-Dawley rats were ordered from Charles River (Wilmington, MA, USA), housed in groups of two and given 5 days to acclimate to the housing facility. The rats were maintained under standard laboratory conditions with a 12/12 h light/dark cycle and free access to food and water. Twelve adult female Sprague-Dawley rats (270–300 g) were used in our experiments. All rats were deeply anesthetized with intraperitoneal ketamine–xylazine cocktail (80 mg/kg of ketamine, 5 mg/kg of xylazine). Subcutaneous Buprenorphine (0.1 mg/kg of Buprinex) was given before surgery for analgesia. Under a dissecting microscope, the skin and muscles overlying the thoracic cord were separated and retracted, the thoracic level 9 (T9) vertebrae was removed by laminectomy, exposing the underlying spinal cord segment. The rats were kept on a heating pad maintained at 37 °C during surgery. The spinal cord was contused using the Infinite Horizons Spinal Cord Impactor at a force setting of 150 kdyn where the mean actual forces were 151.8 kdyn (range 149–155) and 152.2 kdyn (range 149–155) for rUC-MSCs and control groups, respectively. The mean tissue displacements were 1102 U (range 950–1320 U) and 1188 U (range 960–1350) for rUC-MSCs and control groups, respectively. The incision was sutured closed and the animals were kept on a thermostatically regulated heating pad for 3 days. All surgeries were performed by FMM and BKC. An indelible (permanent) nontoxic marker was used to write identification number on tails and repeat marking was made every 3–4 days as necessary. The bladder of all rats was emptied manually three times per day until recovery of urinary function.

Behavioral assessment

The restoration of motor function following spinal cord contusion was observed by open-field Basso, Beattie, and Bresnahan (BBB) locomotor score [11]. The scale used for measuring hind-limb function with these procedures range from a score of 0, indicating no spontaneous movement, to a maximum score of 21, with an increasing score indicating the use of individual joints, coordinated joint movement, coordinated limb movement, weight-bearing, and other functions. Behavioral testing was performed weekly for 14 weeks after SCI. Two independent investigators, blinded to the animal groups, observed the hind-limb movements in an open field for 5 min after the rats were gently adapted to the field. The scores from the two observers (By YY and WW) were averaged, as well as the scores from the left and right limbs.

Cell transplantation

Rats with BBB locomotor scores of 6–7 1-week post injury were used to ensure that all animals had the same severity of injury. The rats were randomly assigned (By MAA) to two groups with six rats each and injected with either (1) 1 ml ringer-lactate saline (RL) or (2) rUC-MSCs (2×10^6 cells suspended 1 ml of RL solution) through the tail vein using a 1 ml syringe (McKesson Medical-Surgical, Richmond, VA) with a 25 G needle over a 5 min period.

Tissue processing and histology

The spinal cord was prepared for tissue evaluation after 14 weeks post injury. All the rats were deeply anesthetized with a ketamine–xylazine cocktail (80 mg/kg of ketamine, 10 mg/kg of xylazine) and then perfused transcardially with 0.01 M PBS (pH 7.4), followed by 4% paraformaldehyde (PFA) in 0.01 M PBS. The whole vertebral column was removed en-block and post-fixed in 4% PFA for 3 days. The spinal cord was then dissected out and segments 10 mm rostral and caudal to injury site were then embedded in paraffin, and serially sectioned into 10-µm-thick transverse sections for histopathologic analysis and immunostaining. All sectioned were examined blindly (By YY and WW).

Histopathology—hematoxylin and eosin (H&E) staining and cavity measure

The sections were then observed under a light microscope to assess tissue morphology and determine the injury site. Nine 10 µm coronal sections 500 µm apart rostral and caudal of lesion epicenter were analyzed for H&E staining. The size of the cavity was divided by the total size of the spinal cord section and was presented as percentages using ImageJ software (Wayne Rasband, National Institute of Health, USA).

Immunofluorescence

Three 10 µm sections from each rat were selected from the injury epicenter, 1000 µm rostral and 100 0µm caudal. The sections were deparaffinized using serial washes of xylene and ethanol. The sections were then rehydrated, and antigen retrieval was performed using a 1 mM EDTA solution.

Next, the sections were washed three times with PBS followed by blocking in 10% normal donkey serum in a 0.1% Triton-X in PBS for 30 min. Following blocking, sections were incubated in primary antibody diluted in blocking buffer overnight at 4 °C. Primary antibodies used were mouse anti-β tubulin (1:300, Millipore), rabbit antimyelin basic protein (MBP, 1:400, Abcam) or mouse anticchondroitin sulfate proteoglycan (CSPG, 1:200, Abcam) and rabbit antiglial fibrillary acidic protein (GFAP, 1:1600, DAKO). The next day, the sections were washed 3 times with PBS and incubated in donkey antirabbit Cy3 (1:200, Jackson Immunoresearch) and donkey antimouse Cy2 (1:200, Jackson Immunoresearch) for 1 h at room temperature. Sections were then washed 3 times in PBS, mounted with SlowFade mounting medium with DAPI (Life technology, USA) using a glass coverslip. Images were captured using standard fluorescent microscope (Zeiss, Germany).

Myelinated axon measurement

Axon myelination was measured by counting the number of β tubulin positive axon with an MBP ring. Myelinated axons were counted from whole spinal column for each sample by two individuals (FMM & YY). All the analyses were performed under blinded conditions.

Astrogliosis and glial scar measurement

Astrogliosis was measured using GFAP immunostaining and glial scar formation was measured using CSPG. Only injury epicenter, 1000 µm rostral and 1000 µm caudal sections were used for each sample. Images were taken on a standard fluorescent microscope (Zeiss, Germany) at excitation of 550 nm and emission at 570 nm for GFAP and at excitation of 492 nm and emission at 510 nm for CSPG. Although the animals were randomized, we had animals from both groups at each of the experiments so that the differences in staining would average out over the groups. The pixel intensity (mean gray value) was measured using ImageJ and then the mean background intensity was subtracted. In addition, we measured the percentage of GFAP and CSPG positive area from the section of whole spinal cord using ImageJ.

Statistical analysis

Data are presented as mean values ± standard deviation (SD). Quantitative data from BBB scores were evaluated for statistical significance by two-way analysis of variance. Differences among groups were assessed by two samples student's t test to identify individual group differences. Differences were deemed statistically significant at $p < 0.05$.

Results

Behavioral assessment

We examined intravenous delivery of rUC-MSC for treatment of SCI. The mean (SD) BBB scores at week one post SCI of rUC-MSC was 7.0 ± 0.3 and control group was 6.5 ± 0.6. There mean difference (95% CI) between the two groups was 0.53 (−0.19 to 1.25) and the difference was not found to be significant ($p > 0.99$). Animals received an intravenous dose of 2 million rUC-MSC or 1 ml RL at 1-week following contusive SCI. RL treated animals recovered from hind-limb paralysis to a mean (SD) BBB score of 8.6 ± 1.2 at 2 weeks post injury, which corresponds to the ability to sweeping or planter placement of the paw with no weight support (Fig. 1a). rUC-MSC treated rats 2 weeks post injury had significant improvements in locomotion (Fig. 1a) with a mean (SD) BBB score of 11.8 ± 1.2, corresponding to consistent hind-limb stepping with occasional coordination between the four limbs. The mean difference (95% CI) between the two groups at 2 weeks post SCI was found to be 3.2 (1.45–4.87), and the difference was found to be statistically significant ($p < 0.05$). The hind-limb function of rUC-MSC treated rats remained significantly greater than the control throughout the whole course of the experiment, suggesting a strong neuroprotective effect. At 14 weeks after SCI, the BBB scores were 14.6 ± 1.9 and 10.1 ± 1.7 for the treated and control groups, respectively. The mean difference (95% CI) in BBB score between the two groups at 14 weeks post SCI was found to be 4.55 (2.04–7.06), and the difference was found to be statistically significant ($p < 0.001$) (Fig. 1a).

Measurement of the cavity volume

The secondary injury cascade triggered by SCI leads to the formation of a large cavity, which spreads in both rostral and caudal directions from the lesion epicenter. We quantified the lesion cavity by H–E staining (Fig. 1b). Rats treated with rUC-MSCs had a significantly reduced cavity size in the injury epicenter compared to controls (control: 33.0% ± 2.1 UCMSC: 25.3% ± 3.8, $p < 0.05$). The mean difference (95% CI) in cavity size between the two groups was found to be 7.7% (−12.3 to −2.98). In the rUC-MSC treated group for sections 500, 1000, 1500, and 2000 µm caudal to the injury epicenter, the cavity sizes were 5.7% ± 4, 3.7 ± 2, 2.7% ± 1.2, and 1.4% ± 1.4, respectively, while in control group they were 21.3% ± 10.1, 13.3% ± 7.4, 13.0% ± 1.6, and 7.6% ± 1.9, respectively. The mean differences (95% CI) between the two groups for sections 500, 1000, 1500, and 2000 µm caudal to the injury epicenter were found to be15.7 (−45.7 to 14.4), −9.7 (−28.1 to 8.8), −10.3 (−12.4 to −8.1), and −6.2 (−11.3 to −1.1),

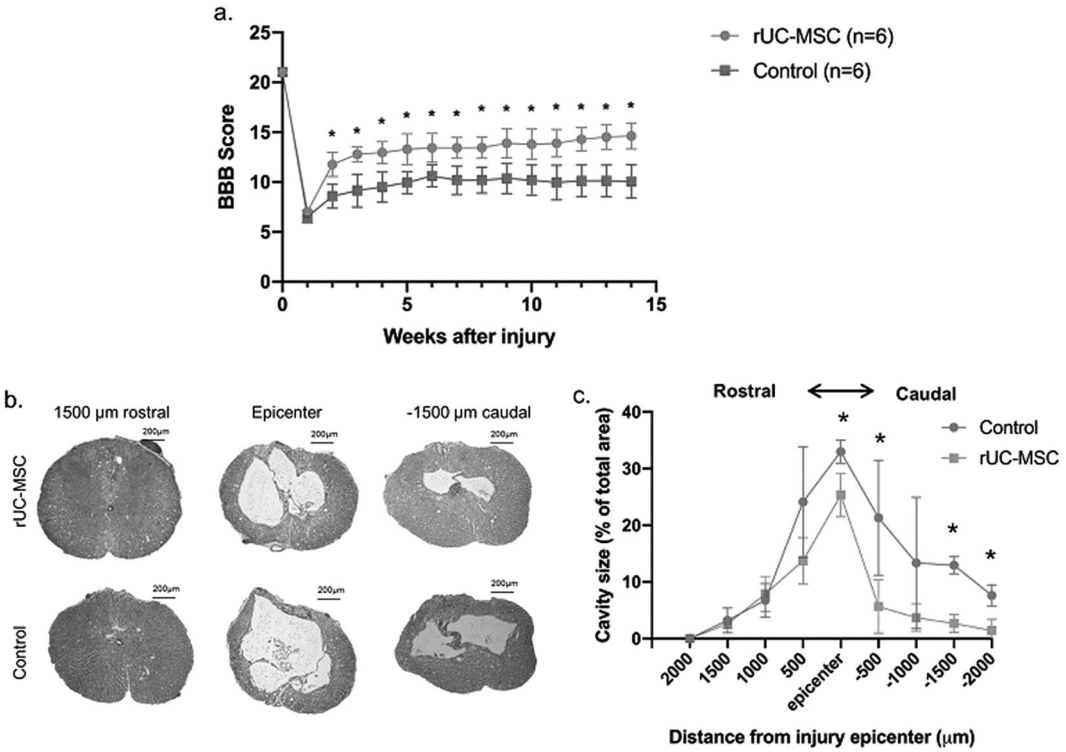

Fig. 1 Improvement in hind-limb locomotor function as measured by the BBB motor score following rUC-MSC treatment of rats with T9 contusion. a Locomotor performance was evaluated using the BBB locomotor rating scale (0–21). Rats with the BBB score between 6 and 7 were treated to ensure all the rats were of similar severity of injury. SCI rats were treated with rUC-MSCs or vehicle at 7 days post injury. Rats treated with rUC-MSCs exhibited significant improvement in locomotor function as early as 2 weeks post injury and this improvement persisted over 14 weeks as compared to controls (*$p < 0.05$). **b** Cavity size was measured using H&E staining of spinal cord 14 weeks post injury in rUC-MSC treated and control rats. **c** Treatment with rUC-MSC reduced the cavity size at injury epicenter and caudal to the injury when compared with control (*$p < 0.05$), however, the same effect was not seen rostral to the injury.

respectively. The reduced cavity size persisted caudal to the injury when compared to the control but not rostral to the injury (Fig. 1c).

Myelination in the lesion zone

To examine whether the rUC-MSC intravenous administration had more myelinated axons, we looked at co-staining of β tubulin and MBP (Fig. 2a–e). A loss of myelinated axon was apparent in the control group; myelinated axons: 42 ± 8.9, 10 ± 1.7, and 25.6 ± 8.1 axons 1000 µm rostral, epicenter, and 1000 µm caudal of the injury respectively compared to the rUC-MSC treated group (myelinated axons: 46.7 ± 9.0, 18.3 ± 4.0, and 41.3 ± 9.0 in 1000 µm rostral, epicenter, and 1000 µm caudal of the injury, respectively (Fig. 2f). The mean differences (95% CI) between the two groups for sections 1000 µm rostral, epicenter, and 1000 µm caudal of the injury were found to be 4.7 (41.0 to −31.7; $p < 0.5$), 8.3 (18.7 to −2.0; $p < 0.05$), and 15.7 (42.9 to −11.6; $p < 0.08$), respectively. Following rUC-MSC treatment, the number of unmyelinated axons had no significant change but the total axon count had significant increase at 1000 µm caudal of the injury epicenter (total axon count: 104.7 ± 6.4) compared to the control (total axon count: 74.5 ± 7.1; $p < 0.001$) (Fig. 2g, h). The mean differences (95% CI) of total axon count at 1000 µm caudal of the injury epicenter between the two groups was found to be −30.2 (−26.2 to −34.2), $p < 0.01$.

Astrogliosis and glial scar

The upregulation of GFAP has been shown to be the hallmark of reactive astrocytes after neurotrauma [12]. Treatment with rUC-MSC significantly reduced the intensity of GFAP at the injury epicenter 14 weeks after SCI as compared with that of the vehicle control (72.4 ± 3.7 vs 85.7 ± 4.7 ($p < 0.05$) while 1000 µm rostral and caudal had no significant difference (Fig. 3a–c). The mean differences (95% CI) of GFAP intensity at injury epicenter between the two groups were found to be −13.3 (−10.8 to −15.9).

We examined the intensity of CSPG in order to measure the glial scar formation (Fig. 3d, e). Mean CSPG intensity was significantly reduced at 1000 µm caudal to injury epicenter in rUC-MSC group when compared to the control group (53.8 ± 5.2 vs 70.1 ± 1.6, $p < 0.05$) while 1000 µm rostral and epicenter had no significant difference (Fig. 3f).

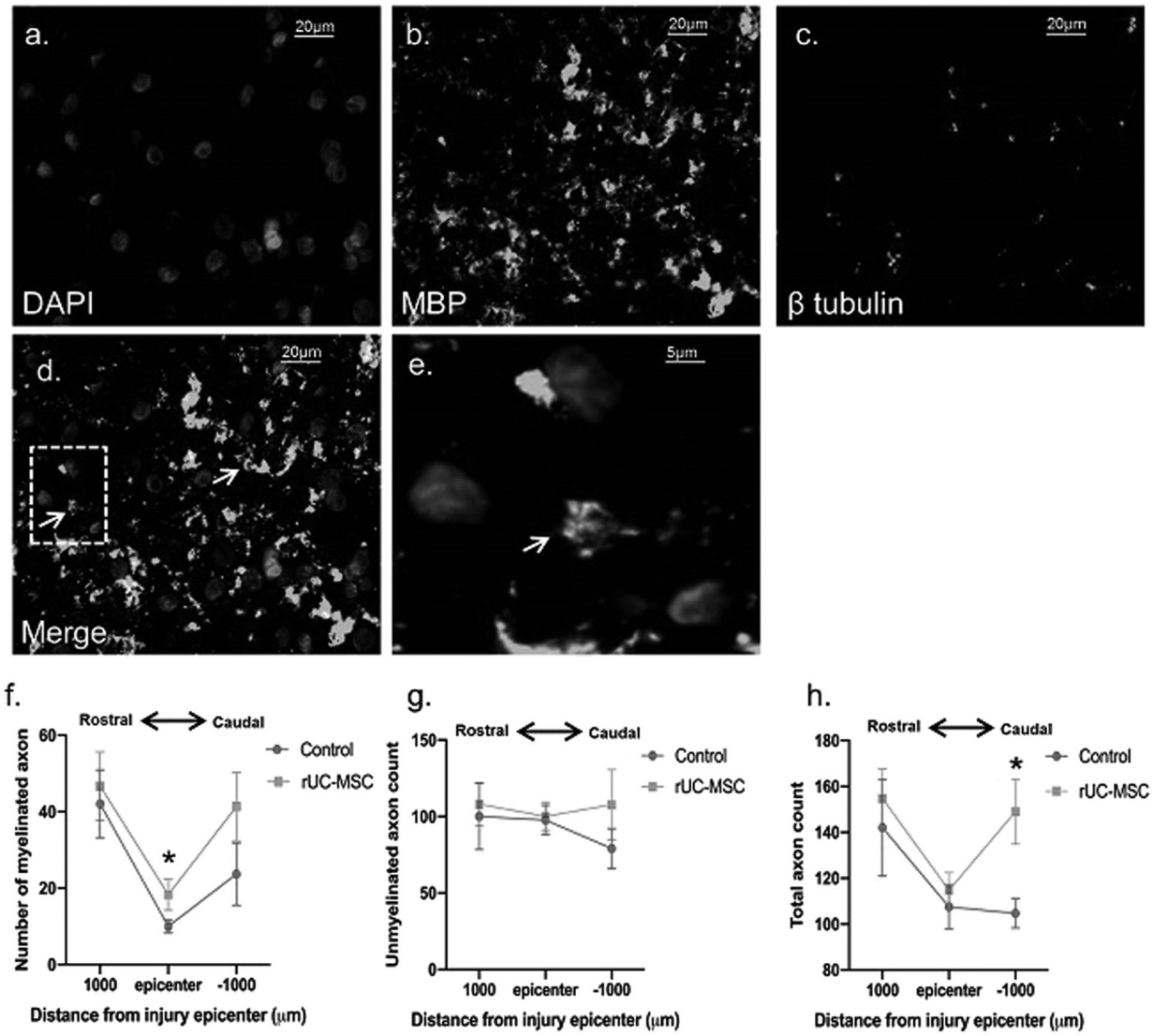

Fig. 2 Quantification of myelinated axons 14 weeks post injury following rUC-MSC treatment. 10 μm-thick transverse paraffin sections of treated and vehicle spinal cords were stained with DAPI ((**a**) blue), β-tubulin ((**b**); green), and myelin basic protein ((**c**) MBP; orange). **d** Axon myelination was visualized and counted using immunofluorescence of β-tubulin (green) co-stained with myelin basic protein (MBP; orange). **e** Magnification of the white box in (**d**) illustrates the characteristic staining pattern of myelinated axons that have a punctate axon surrounded by an MBP ring (white arrow). Quantitative analysis represented the rUC-MSC treated group had significantly greater number of myelinated (**f**), unmyelinated (**g**) and total (**h**) axons in injury epicenter compared with control group. **g** Data presented were axon count ±SD (*$p < 0.05$).

The mean differences (95% CI) of CSPG intensity at injury epicenter between the two groups were found 16.8 (0.6 to −33.0).

In addition, we found a similar trend of % change in positive GFAP and CSPG stain between the two groups (Supplementary Fig. 3a, b).

Discussion

In the present study, we demonstrated that intravenous administration of rUC-MSCs in a contusive SCI rat model resulted in greater number of myelinated axons, reduced cavity size, reduced astrogliosis, and reduced scar formation, all of which lead to improved hind-limb function that could be sustained over 14 weeks. To date, a multitude of experimental treatments have been developed to address the regenerative and restorative ability of the spinal cord [13]. Cellular therapy has been purported to be a promising area of research for SCI. Among the various types of cellular therapies investigated [3, 14, 15], UC-MSCs have recently been shown to hold significant therapeutic potential for the treatment of SCI. A recent study demonstrated that human umbilical cord-derived perivascular cell-infusion

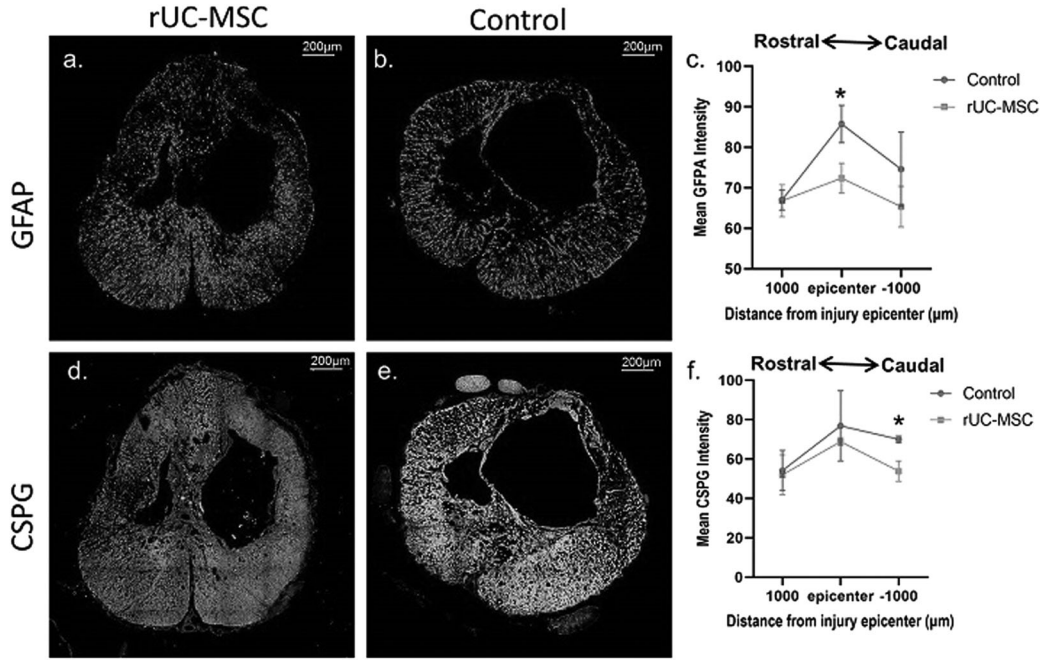

Fig. 3 Quantification of astrogliosis and glial scarring using GFAP and CSPG staining of 10 μm thick transverse spinal cord sections 14 weeks post SCI. a, **b** Astrogliosis was measured using glial fibrillary acidic protein (GFAP) immunostaining and, **d**, **e** Glial scar formation was measured by staining of chondroitin sulfate proteoglycan (CSPG; green). **c**, **f** rUC-MSC administration reduced glial scar and astrogliosis at injury epicenter compared with control. Data were mean intensity ±SD (*$p < 0.05$).

outperformed commercially available bone marrow derived MSCs and conferred long-term functional recovery [16]. Our rat contusive SCI model showed early and sustained functional improvement after intravenous administration when treated subacutely. This may indicate that rUC-MSCs exert their benefit through a neuroprotective mechanism early after treatment, an effect that persisted through the 14 weeks course.

A chronic and progressive demyelination of spared axons is one of the most important secondary pathological processes following SCI which restrains functional recovery [17]. In our rat SCI model, we found that the greater amount of remaining myelin sheath in the injured spinal cord treated with rUC-MSCs was consistent with the functional recovery. The greater number of myelinated nerve fibers may be due to axonal re-myelination, axonal regeneration or the survival of neural fibers with a conserved myelin sheath. Interestingly, we observed greater number of myelinated axon caudally than in the injury epicenter. This might have resulted from modulation of the macrophage activity to prevent the axonal die back [18]. A more detailed investigation of the effects of rUC-MSCs on these processes will be required to fully understand the underlying mechanism. Zhilai et al. [10] found a significant increase in axonal preservation associated with a reduction in inflammatory activity resulting in functional improvement following SCI after human UCMSC transplantation in a rat contusion SCI model. This suggested that UCMSC transplantation provides a microenvironment favorable for cell survival, tissue repair and functional recovery [10]. In chronic SCI, the glial scar consists of inhibitory molecules, such as chondroitin and keratan sulfate proteoglycans, that may play a crucial role in regenerative failure [19, 20]. We found that rUC-MSCs treated rats had less astrogliosis and glial scar at the injury site compared to control rats at 14 weeks post injury. This result may support the persistent functional improvement in rats treated with rUC-MSCs. Overall, the improvement in gait following rUC-MSC treatment was associated with greater number of myelinated axons, decreased astrogliosis, and reduced CSPG scar formation. The current favored hypothesis is that the injected cells work via a paracrine mechanism, secreting factors that help damaged tissue recover [21]. However, inclusion of dead cell transplantation as a control could possibly elucidated this mechanism.

Despite several effective cellular therapies in preclinical studies for SCI, it is still unclear which route of administration would be the most effective. Compared to more invasive techniques of delivery such as intrathecal or intraspinal implantation, IV injection offers a minimally invasive method of cell delivery. Osaka et al. showed that systemic infusion of bone marrow derived MSC into rats following contusive SCI resulted in increased local BDNF levels, reduction in spinal cord lesion volume, and improved functional outcomes [22]. They also observed that MSC infusions at 6 h, 1 and 3 days had the greatest

functional recovery [22]. Our study demonstrates that intravenously injected MSCs at 7 day post injury were effective in enhancing functional recovery following SCI. This result suggests a wider range of effective interventional timepoints to utilize intravenous UCMSC administration. Similarly, a previous study by White et al. also observed functional recovery in mice receiving IV injection of mesenchymal progenitor cells on day 1 following a contusion of the cervical spine. They demonstrated that the cells distributed solely to the lungs and not the spinal cord [23]. Thus, we could hypothesize that any beneficial effects observed post injection occurred systemically.

Several clinical trials have used autologous cells for transplantation following SCI; however, this increases the amount of time required before the cells can be administered. They must be isolated from patients and then cultured in large quantities. In addition, there is a risk of batch failure or failure to reach an adequate amount of cells thereby delaying the intervention. This could be circumvented by the use of allogeneic cells, which allows for development and freezing of optimal cell lines in advance. In our study, we used MSCs isolated and cultured from rat umbilical cord of the same species. These cells were then frozen and used on demand, being drawn up at the time of administration. This procedure allowed for standardization of the cell type used as well as we were able to receive the cells overnight from a central facility demonstrating this method would be feasible for use in patients where a cell dose could be delivered to any hospital from a central facility thereby reducing costs, center to center variability, and the need for an institutional GMP cell facility.

In order to validate human cells for use in the clinic, studies are done using xenogeneic injections into rodents. One drawback to the use of xenogeneic cells is that immunosuppression is required to reduce rejection. In our study, we used MSCs derived from rat which allowed us to investigate if infusion of allogeneic cells without use of any immunosuppression drugs is effective. Use of immunosuppress drugs, such as cyclosporine, in experimental animal models is a common method to reduce the immune reaction for any cellular therapy derived from different species or from other animals. Interestingly, considerable evidence has shown that cyclosporin A (CsA) may have neuroprotective properties by inhibiting both the inflammatory reaction and the synthesis of nitric oxide [24]. On the other hand, few studies found that CsA did not aid in reducing tissue damage following contusion SCI [25, 26]. Therefore, without using immunosuppressive drugs, our study had reduced the influence of outside cofactors and represented specifically effects of UCMSC. In addition, use of allogeneic UCMSC provides clear clinical translational information regarding the use of allogeneic UCMSC in human. With growing developments in MSC applications, recognizing the optimal cell source and delivery method depending on SCI conditions is vital to clinical translation. We show that a minimally invasive intravenous UCMSC transplantation procedure significantly improved the motor function in rats with spinal cord contusion injury. Thus, we have provided a novel strategy to improve SCI treatment by utilizing UC-MSCs, suggesting a promising line of therapy in future clinical practice.

Data availability

The datasets generated and/or analysed during the current study are available in Supplementary Table 1.

Acknowledgements We thank the Neuro-Informatics laboratory (Mayo Clinic) for general technical support.

Funding This work was partially supported by funding from Sabes foundation.

Author contributions FMM: collection and assembly of data, data analysis and interpretation, paper writing. YY: collection and assembly of data, data analysis and interpretation, paper editing. WW: collection and assembly of data, data analysis and interpretation. AMS: Data analysis and interpretation, paper editing. BKC: collection and assembly of data. MAA: collection and assembly of data, paper editing. AG: collection and assembly of data, paper editing. JJN: collection of data. AJW: data interpretation, paper editing. J-CY: collection and assembly of data, paper editing. KP: conception and design, paper editing. MB: conception and design, data interpretation, paper editing.

Compliance with ethical standards

Conflict of interest The authors declare that they have no conflict of interest.

Ethical approval All animal protocols were approved by the Mayo Clinic Institutional Animal Care and Use Committee and complied with guidelines from the National Institutes of Health (Protocol #A2553-17). We certify that all applicable institutional and governmental regulations concerning the ethical use of animals were followed during the course of this research.

References

1. Ramadan WS, Abdel-Hamid GA, Al-Karim S, Abbas AT. Histological, immunohistochemical and ultrastructural study of secondary compressed spinal cord injury in a rat model. Folia Histochem Cytobiol. 2017;55:11–20.
2. Holmes D. Spinal-cord injury: spurring regrowth. Nature. 2017; 552:S49.
3. Assinck P, Duncan GJ, Hilton BJ, Plemel JR, Tetzlaff W. Cell transplantation therapy for spinal cord injury. Nat Neurosci. 2017; 20:637–47.
4. Jin MC, Medress ZA, Azad TD, Doulames VM, Veeravagu A. Stem cell therapies for acute spinal cord injury in humans: a review. Neurosurg Focus. 2019;46:E10.

5. Nagoshi N, Okano H. Applications of induced pluripotent stem cell technologies in spinal cord injury. J Neurochem. 2017;141:848–60.
6. Shende P, Subedi M. Pathophysiology, mechanisms and applications of mesenchymal stem cells for the treatment of spinal cord injury. Biomed Pharmacother. 2017;91:693–706.
7. Yang C, Wang G, Ma F, Yu B, Chen F, Yang J, et al. Repeated injections of human umbilical cord blood-derived mesenchymal stem cells significantly promotes functional recovery in rabbits with spinal cord injury of two noncontinuous segments. Stem Cell Res Ther. 2018;9:136.
8. Ning G, Tang L, Wu Q, Li Y, Li Y, Zhang C, et al. Human umbilical cord blood stem cells for spinal cord injury: early transplantation results in better local angiogenesis. Regen Med. 2013;8:271–81.
9. Veeravalli KK, Dasari VR, Tsung AJ, Dinh DH, Gujrati M, Fassett D, et al. Human umbilical cord blood stem cells upregulate matrix metalloproteinase-2 in rats after spinal cord injury. Neurobiol Dis. 2009;36:200–12.
10. Zhilai Z, Biling M, Sujun Q, Chao D, Benchao S, Shuai H, et al. Preconditioning in lowered oxygen enhances the therapeutic potential of human umbilical mesenchymal stem cells in a rat model of spinal cord injury. Brain Res. 2016;1642:426–35.
11. Basso DM, Beattie MS, Bresnahan JC. A sensitive and reliable locomotor rating scale for open field testing in rats. J Neurotrauma. 1995;12:1–21.
12. Pekny M, Pekna M. Reactive gliosis in the pathogenesis of CNS diseases. Biochim Biophys Acta—Mol Basis Dis. 2016;1862:483–91.
13. Dalamagkas K, Tsintou M, Seifalian A, Seifalian AM. Translational regenerative therapies for chronic spinal cord injury. Int J Mol Sci. 2018;19:1776.
14. Ryu HH, Kang BJ, Park SS, Kim Y, Sung GJ, Woo HM, et al. Comparison of mesenchymal stem cells derived from fat, bone marrow, Wharton's jelly, and umbilical cord blood for treating spinal cord injuries in dogs. J Vet Med Sci. 2012;74:1617–30.
15. Filous AR, Schwab JM. Determinants of axon growth, plasticity, and regeneration in the context of spinal cord injury. Am J Pathol. 2018;188:53–62.
16. Vawda R, Badner A, Hong J, Mikhail M, Lakhani A, Dragas R, et al. Early Intravenous infusion of mesenchymal stromal cells exerts a tissue source age-dependent beneficial effect on neurovascular integrity and neurobehavioral recovery after traumatic cervical spinal cord injury. Stem Cells Transl Med. 2019;8:639–49.
17. Kim SU, de Vellis J. Stem cell-based cell therapy in neurological diseases: a review. J Neurosci Res. 2009;87:2183–200.
18. Horn KP, Busch SA, Hawthorne AL, van Rooijen N, Silver J. Another barrier to regeneration in the CNS: activated macrophages induce extensive retraction of dystrophic axons through direct physical interactions. J Neurosci. 2008;28:9330–41.
19. Silver J, Miller JH. Regeneration beyond the glial scar. Nat Rev Neurosci. 2004;5:146–56.
20. Silver J. The glial scar is more than just astrocytes. Exp Neurol. 2016;286:147–9.
21. Cofano F, Boido M, Monticelli M, Zenga F, Ducati A, Vercelli A, et al. Mesenchymal stem cells for spinal cord injury: current options, limitations, and future of cell therapy. Int J Mol Sci. 2019;20:2698.
22. Osaka M, Honmou O, Murakami T, Nonaka T, Houkin K, Hamada H, et al. Intravenous administration of mesenchymal stem cells derived from bone marrow after contusive spinal cord injury improves functional outcome. Brain Res. 2010;1343:226–35.
23. White SV, Czisch CE, Han MH, Plant CD, Harvey AR, Plant GW. Intravenous transplantation of mesenchymal progenitors distribute solely to the lungs and improve outcomes in cervical spinal cord injury. Stem Cells. 2016;34:1812–25.
24. Diaz-Ruiz A, Vergara P, Perez-Severiano F, Segovia J, Guizar-Sahagun G, Ibarra A, et al. Cyclosporin-A inhibits constitutive nitric oxide synthase activity and neuronal and endothelial nitric oxide synthase expressions after spinal cord injury in rats. Neurochem Res. 2005;30:245–51.
25. McMahon SS, Albermann S, Rooney GE, Moran C, Hynes J, Garcia Y, et al. Effect of cyclosporin A on functional recovery in the spinal cord following contusion injury. J Anat. 2009;215:267–79.
26. Rabchevsky AG, Fugaccia I, Sullivan PG, Scheff SW. Cyclosporin A treatment following spinal cord injury to the rat: behavioral effects and stereological assessment of tissue sparing. J Neurotrauma. 2001;18:513–22.